

**DYNAMIC STRUCTURES AND MIXING PROCESSES IN SUB- AND SUPERSONIC HYDROGEN/AIR FLAMES IN COMBUSTION CHAMBERS WITH CASCADES OF REARWARD FACING STEPS**

W. Gabler, M. Haibel, F. Mayinger  
 Lehrstuhl A für Thermodynamik  
 Technische Universität München  
 80290 München  
 Germany

Abstract

The influence of turbulent structures and shock patterns on the mixing and combustion processes in sub- and supersonic hydrogen/air flames was investigated in a multistep combustor with cascades of rearward facing steps. The turbulent structures and the concentration profiles in the mixing jet and in the reaction zone of the flame was investigated by means of non-intrusive optical measurement techniques. The experiments showed that rearward facing steps and multistep fuel injection generate vortices in the mixing jet which enhanced the mixing and combustion processes. Due to this it was possible to achieve a higher penetration and a larger thickness of the mixing jet compared with single-step injection. Rearward facing steps and multistep fuel injection were also used to stabilize the flames and to shorten the flame length. The evaluation of the experimental data led to new formulae which predict the development and the concentration profile of the mixing jet in sub- and supersonic hydrogen/air flames.

Nomenclature

$A_e$  entrance cross section of the combustion chamber  
 $C$  constant in equation (1)  
 $c_{max}$  concentration of helium on the trajectory  
 $c_{He}$  concentration of helium in the mixing jet  
 $d_0$  diameter of the injection hole  
 $K$  constant in equation (7)  
 $m_{air}$  mass flow of the main air stream  
 $m_{fuel}$  mass flow of the fuel  
 $m_{He}$  mass flow of the helium  
 $m_{H_2}$  mass flow of the hydrogen  
 $Ma_{air}$  initial air Mach number  
 $T_0$  total temperature in the initial air stream  
 $x$  coordinate in the direction of the initial air flow field  
 $x_T$  coordinate of the maxima in the trajectory

$x'$  coordinate on the trajectory  
 $x_p$  coordinate on the trajectory which indicates the beginning decrease of concentration  
 $y$  coordinate normal to the direction of the initial air flow field  
 $y'$  coordinate on the trajectory

Greek symbols

$\xi_{He}$  ratio of specific mass flow rates of helium calculated by equation (2)  
 $(\rho w)_{air}$  specific mass flow rate of air  
 $(\rho w)_{He}$  specific mass flow rate of helium  
 $(\rho w)_{He,crit}$  critical specific mass flow rate of helium

1. Introduction

The development of sub- and supersonic combustion chambers for aircraft propulsion system is guided by the demand of combustion chamber of limited length together with high fuel efficiency. In the combustor chemical reaction can only occur if the reactants are molecularly mixed. In this context, one of the major topics is the optimization of the mixing process, because of its keyrole for both development aims mentioned above. The mixing process itself is influenced by shocks and expansion waves and turbulent structures in the flow field of the combustion chamber [1]. These structures are originated by the injector geometry and the injected fuel jet.

Figure 1 shows the supersonic flow ( $Ma_{air}=2.1$ ) in the vicinity of a backward facing step without fuel injection monitored by means of shadowgraph. This picture depicts a Prandtl-Meyer expansion which is originated due to the expansion after the attachment point of the back step. A shear layer emanating from the separation point of the rearward facing step and its reattaching on

the chamber wall can be clearly seen. Because of the change in the flow direction after the backward facing step a recompression shock is travelling from the reattachment point of the shear layer.

Figure 2 shows the influence of the injected fuel on the supersonic flow structure. Due to the penetration of the injected fuel an oblique shock was generated in front of the fuel jet. This oblique shock wave was reflected on the upper chamber wall and touched the mixing shear layer. Comparing figure 2 with figure 1 it can be seen that the reattachment point of the shear layer and the



Fig. 1: Flow structure of a supersonic flow over a rearward facing step at  $Ma_{air} = 2.1$

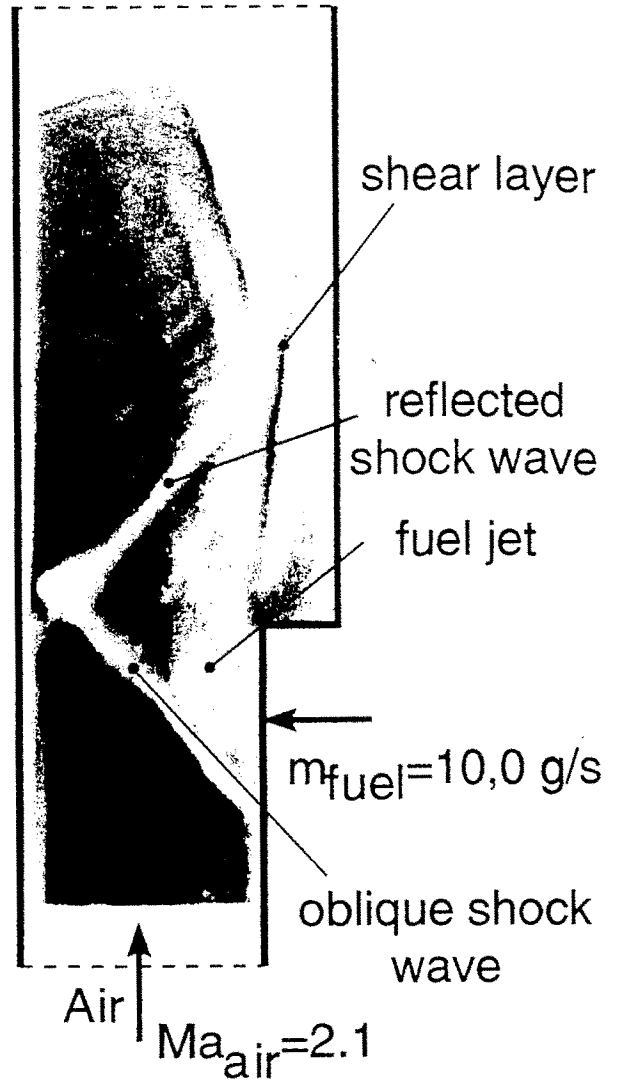


Fig. 2: Supersonic flow field with fuel injection ( $Ma_{air} = 2.1$ ;  $m_{fuel} = 10,0$  g/s)

recompression shock wave shifted downstream when fuel was injected.

Numerous studies are concerned with the analysis of mixing processes of fuel/air in high speed airflows [1-17]. These papers describe the influence of shear layers, expansion fan and shock waves on the mixing process using different injector geometries. Oswald et al [2] analysed the flow field in a supersonic combustor with  $H_2$ -injection through a strut by using particle image displacement velocimetry (PIDV). Schetz et al [18] investigated analytically the structure of gaseous jets which are injected through holes in the combustion chamber wall into a supersonic stream. These papers showed, that eddies, which are induced by local velocity gradients in the flow field, are able

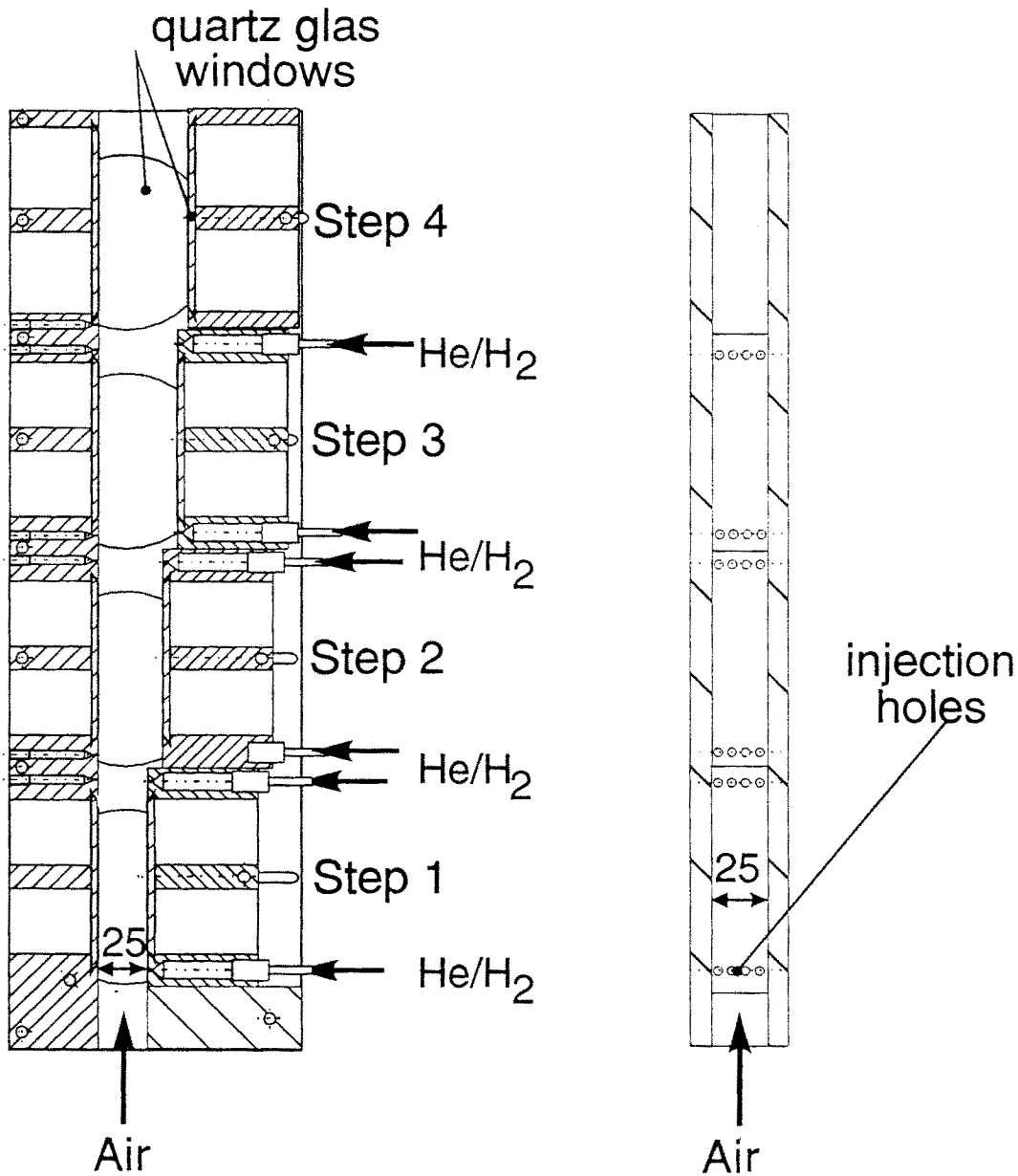


Fig. 3: Multistep combustor

to enhance the mixing process in supersonic combustion chambers.

The intention of this contribution is to provide detailed data about the effect of cascades of rearward facing steps on the mixing and combustion processes. Thereby the influence of flow characteristics like shock patterns and expansion waves on the fuel/air mixing are demonstrated. The influence of multistep fuel injection on the development of mixing and the turbulent structure of sub- and supersonic H<sub>2</sub> flames were also investigated by using non-intrusive optical measurement techniques.

## 2. Experimental Setup and Measurement Techniques

### 2.1 Experimental Setup

The investigation of the mixing processes and the flame structure in sub- and supersonic flow field were performed in a blow down wind tunnel using a single- and multistep fuel injection system. This wind tunnel consisted of a Laval-contour and a multistep combustion chamber. The main airflow was accelerated in the Laval-contour up to a maximum Mach number  $Ma_{air}$  of 2.1. The total temperature  $T_0$  of the airstream was 293 K and the maximum mass flow of the air  $m_{air}$  was 850 g/s. After acceleration the airflow entered the combustion chamber with a entrance cross section of

$A_c = 25 \times 25$  mm. Three downstream rearward facing steps were used in the multistep combustor to generate large scale turbulent structures to receive fine-scale mixing and conditions of flame stability. Due to the height of the steps of 10 mm the exit cross section of the combustor was  $25 \times 55$  mm. Upstream of the steps 1 and 2 fuel was injected either through a single orifice or through a line of injection holes mounted in steps 1-2. The mass flow of the injected fuel was varied from 0 to 10 g/s. All chamber walls were equipped with quartz glass windows to enable the access of optical measurement techniques (i.e. Raman Spectroscopy, laser induced fluorescence, holographic interferometry and shadowgraph technique). Figure 3 shows a sketch of the multistep combustor.

To examine the mixing effects without the influence of chemical processes the fuel/air mixing was investigated in experiments without combustion ('cold mixing') using helium as model gas instead of hydrogen because of safety considerations.

In experiments with combustion the turbulent flame structure and the flame stabilization were investigated by injecting hydrogen.

## 2.2 Measurement techniques

Due to the demand of non-intrusivity for diagnostic techniques in supersonic flows, laser based optical measurement techniques were used to investigate the mixing process and the flame structure in the combustion chamber without perturbing the flow field.

Shadowgraph technique. Shadowgraph technique were used to analyse qualitatively the structure of the highly turbulent flow field. Because of its high sensitivity to density gradients, the method was used to visualize the position of the shock-pattern, the expansion zones, the shear layers and the turbulent fuel jet (Figure 1). This technique is not able to provide information about the concentrations of the species in the mixing layer.

Holographic interferometrie. Holographic interferometrie was employed to investigate the characteristics of the turbulent mass transport in the mixing layer and the structure of the flow field in the combustion chamber by using the 'finite fringe' method. The information about the concentration distribution inside the mixing jet was taken from the deformation of a pattern of originally parallel fringes which is caused due to the injection of helium into the air flow. This process was monitored by using an intensified CCD-camera with a minimal exposure time of 100 ns. By this highly turbulent structures in the mixing zone could be observed.

Furthermore it was also used to measure quantitatively the concentration profile of the mixing jet and the

density distribution in the flow field. Since this technique integrates along the path of light beam, three dimensional effects in the flow field cannot be observed. This also leads to a limited spatial resolution compared with scattering measurements like Raman spectroscopy or Laser-induced fluorescence. More information on the holographic interferometrie is provided in refs. [19-22].

Raman spectroscopy. To gain detailed data about the influence of the shock waves, rearward facing steps and multiple fuel injection on the mixing process, the concentration of all major species at several single points in the mixing area were detected by Raman spectroscopy with high spatial resolution corresponding to a small laser focus. Within the laser focus all molecules are forced to change their rotational/vibrational quantum state emitting scattering light at different wave length which indicate the different species. The concentration profile was received by a spectral analysis of the scattering light with a polychromator and an intensified diode array [23]. Since helium is not a molecule it provides no Ramansignal. Thereby the distribution of helium in the mixing zone was determined by measuring the concentration of the nitrogen. The regarded measurement spots are chosen by consulting the measurements with holographic interferometrie and shadowgraph technique.

Laser induced fluorescence. OH-radicals, which are interim products of the chemical reaction of  $H_2$  and  $O_2$ , indicate the location and extension of the reaction zones. Using laser induced fluorescence (LIF) as measurement technique these OH-radicals are electronically excited due to a thin laser light sheet. After excitation the radicals emit a strong scattering light at the same wave length. Due to the usage of a light sheet it was possible to monitor two dimensional the longitudinal section of the flame structure which is chemically and mechanically frozen because of the extremely short laser pulse width of about 17 ns [23].

## 3. Experimental Results and Discussion

### 3.1 Structure and behaviour of the helium/air mixing jet

To study the mixing effects of fuel and oxidizer in sub- and supersonic airflows without the influence of chemical processes cold experiments using helium as model gas instead of hydrogen were conducted. In order to analyse the effect of multistep injection to the behavior of the mixing jet, the mixing experiments in the cold flow field were subdivided into two parts, single- and multistep fuel injection.

The singlestep injection dealt with the dependency of the fuel/air mixing process on different injector

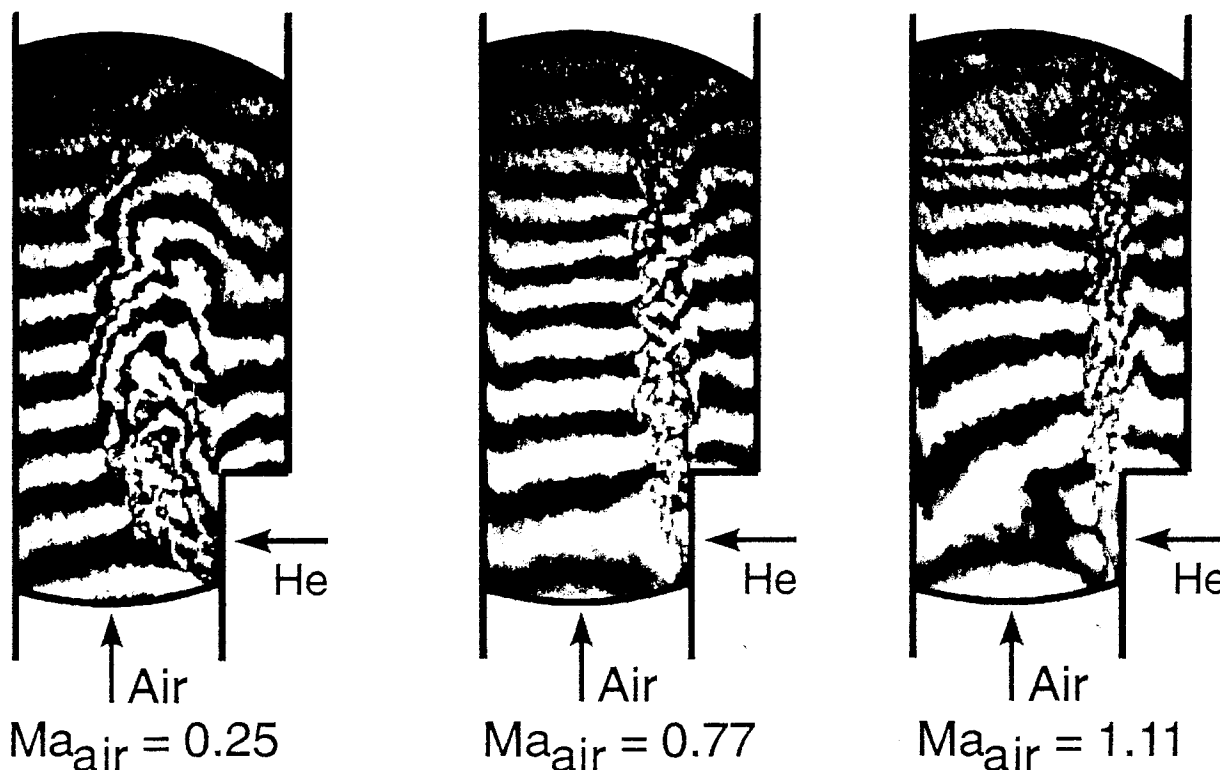


Fig. 4: Influence of the initial air Mach number on the development of the mixing jet monitored by means of holographic interferometry (single hole injector,  $m_{\text{He}} = 1.46 \text{ g/s}$ )

geometries: single hole injector and four hole injector with an injection angle of  $90^\circ$ . This singlestep injection took place up stream of the first rearward facing step. The Mach number of the air flow  $Ma_{\text{air}}$  was varied between 0.25 and 2.1.

Multistep injection, meaning the simultaneous injection of fuel upstream of the first and second rearward facing step, was used to gain a higher mixing rate and a greater thickness of the mixing jet compared with the singlestep injection due to additional vortices in the wake of the jet.

Singlestep fuel injection. Figure 4 shows the effect of the initial air Mach number on the development of the mixing jet monitored by means of holographic interferometry. The fuel was injected perpendicular to the main air flow direction through a single hole in front of the first rearward facing step. The fuel mass flux  $m_{\text{He}}$  was  $1.46 \text{ g/s}$ . It can be seen that an increase of the air Mach number causes a decrease of the penetration and leads to a stronger deflection of the mixing jet, because of the decreasing specific momentum of the helium jet. In addition to this the mixing jet becomes very slender. At  $Ma_{\text{air}} = 1.11$  the fuel jet unites with the free shear layer.

Due to macroscopic and microscopic vortices at  $Ma_{\text{air}} = 0.25$  the outer border of the mixing jet is very ragged. In the supersonic case these eddies are smaller caused by the higher intensity of turbulence. Thereby at  $Ma_{\text{air}} = 1.11$  the outer border of the mixing jet becomes smoother.

Figure 5 depicts the concentration profile which is gained by analysing the interferograms of figure 4. A increase in the air Mach number, the trajectory, which represents the line with the highest helium in the mixing jet, is stronger deflected towards the recirculation zone. Due to smaller eddies the mixing process is suppressed with increasing Mach number. By this the lines with constant helium concentration went further downstream and the mixing jet becomes thinner.

To describe the growth of the outer border and the penetration of the mixing jet, a power law was developed. This law is identical with the one determined by Orth and Funk [24]. The development of the outer border of the mixing jet for the perpendicular helium injection through a single hole is described by equation (1).

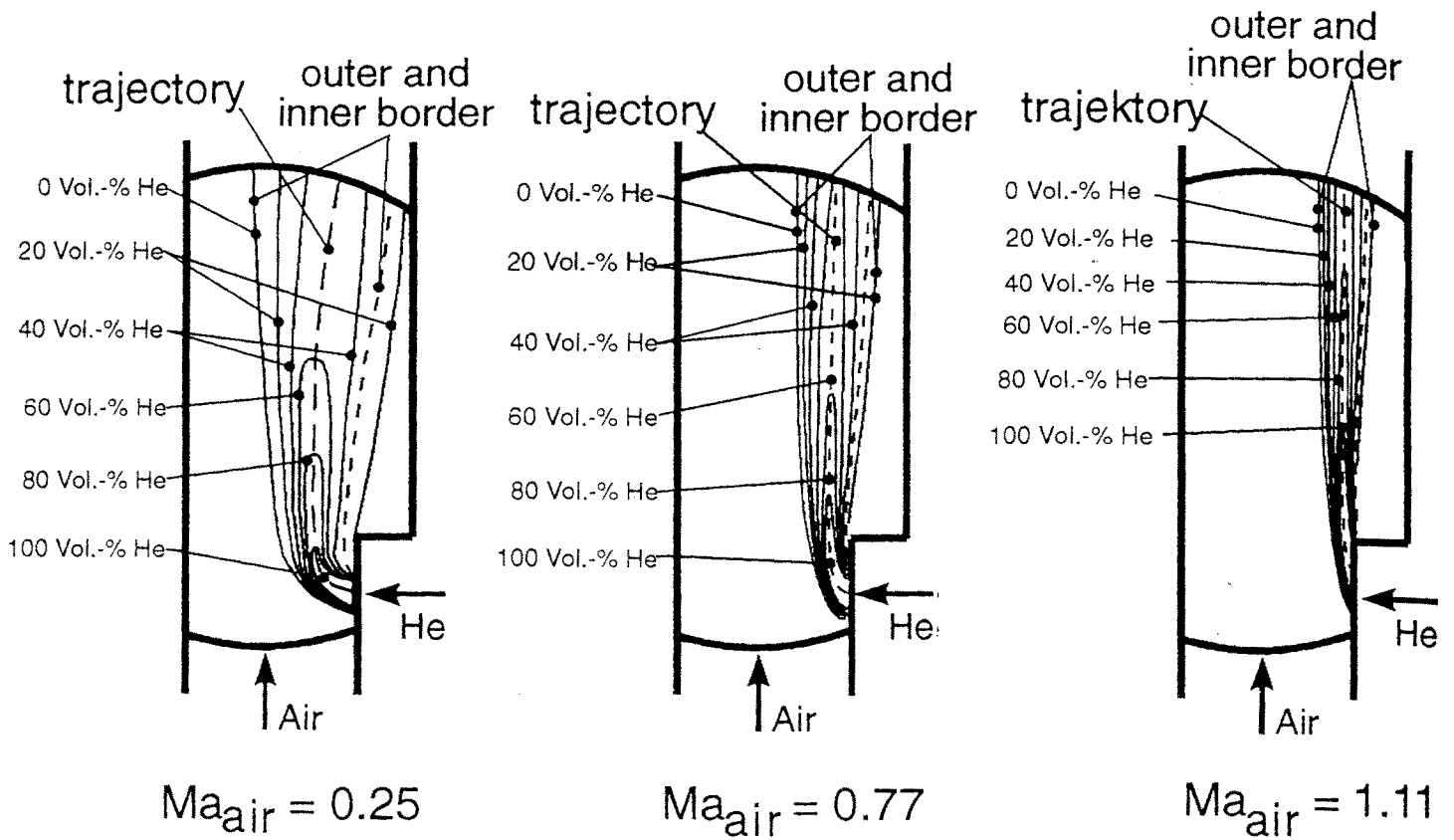


Fig. 5: Influence of the initial air Mach number  $Ma_{air}$  on the concentration profile in the fuel jet ( $\xi_{He} = 1.14$ )

$$\left(\frac{y}{d_0}\right) = 1.6 \cdot \xi_{He}^{0.65} \cdot Ma_{air}^{-1.05} \cdot \left(\frac{x}{d_0} + 0.01\right)^{0.087} \quad (1)$$

The coordinates  $x, y$  are normalized with the injection nozzle diameter  $d_0$ .  $Ma_{air}$  is the initial air Mach number of the main air flow.  $\xi_{He}$  is calculated by equation (2):

$$\xi_{He} = \left(\frac{(\rho w)_{He}}{(\rho w)_{He,crit}}\right) \quad (2)$$

Here  $(\rho w)_{He,crit}$  is the critical specific mass flow which denotes the helium mass flow when the Mach number in the injection nozzle is equal to unity.  $(\rho w)_{He}$  is the actual specific mass flow rate of the injected helium in the experiment. Equation (1) shows that an increasing helium mass flow rate leads to a deeper penetration of the mixing jet into the air flow field. This is indicated by the exponent 0.65 of the specific mass flow rate  $\xi_{He}$ . The fact, that the mixing jet was compressed and the penetration depth decreases with an increasing air Mach number, is considered by the exponent -1.05 of the initial air Mach number  $Ma_{air}$ .

For a better understanding of the nomenclature used in the equations figure 6 shows a sketch of a mixing jet in the vicinity of the fuel injection zone with the outer and inner border of the mixing jet and the coordinate system located in the injector nozzle.

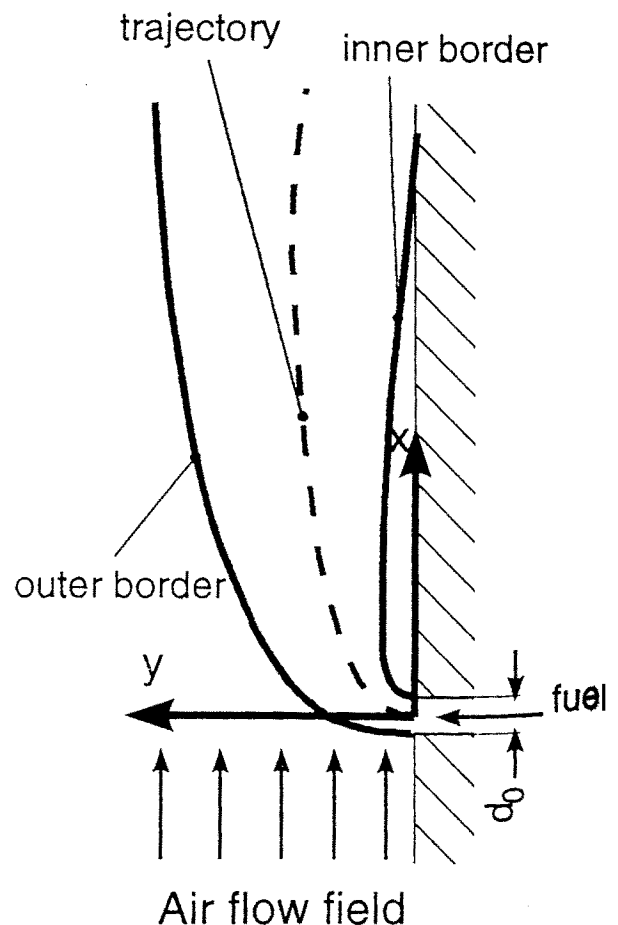


Fig.6: Sketch of the mixing jet in the vicinity of the fuel injection zone

The development of the trajectory can be divided into two parts. Before reaching the point  $x_T$  the trajectory rises towards the centre of the air flow. After this point it falls back towards the recirculation zone. The rising part of the trajectory for single hole injection can be described by the following equation:

$$x \leq x_{T,\max}$$

$$\left(\frac{y}{d_0}\right)_T = 0.5 \cdot \xi_{\text{He}}^{0.72} \cdot \text{Ma}_{\text{air}}^{-1.7} \cdot \left(\frac{x}{d_0}\right)^{0.09} \quad (3)$$

The development of the trajectory after the maximum can be described by equation (4).

$$x > x_{T,\max} \quad (4)$$

$$\left(\frac{y}{d_0}\right)_T = -0.0065 \cdot \xi_{\text{He}}^{-1.3} \cdot \left(\frac{x - x_{T,\max}}{d_0}\right)^2 + \frac{y_{T,\max}}{d_0}$$

with

$$\frac{y_{T,\max}}{d_0} = 0.5 \cdot \xi_{\text{He}}^{0.72} \cdot \text{Ma}_{\text{air}}^{-1.7} \cdot \left(\frac{x_{T,\max}}{d_0}\right)^{0.09} \quad (5)$$

and

$$\frac{x_{T,\max}}{d_0} = 2.8 \cdot \xi_{\text{He}}^{0.7} \cdot \text{Ma}_{\text{air}}^{-1.05} \quad (6)$$

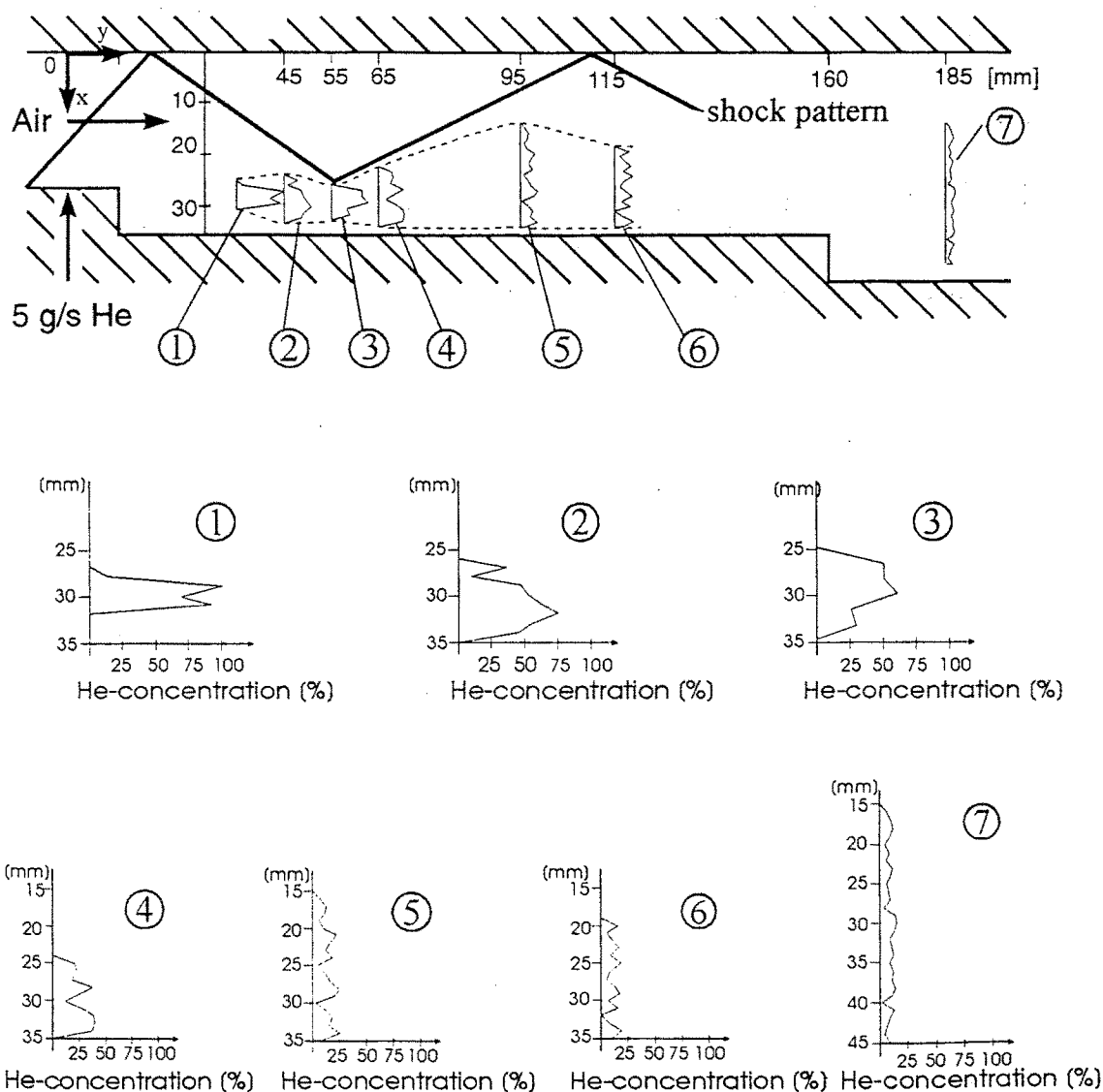


Fig. 7: Influence of shock waves and rearward facing steps on the concentration profile in the mixing jet (four hole injector;  $\text{Ma}_{\text{air}}=2.1$ ;  $m_{\text{He}}=5$  g/s)

The concentration distribution in the mixing jet can be described by using a power law like

$$c_{\text{He}} = c_{\text{max}} \cdot \exp \left[ -K \cdot \left( \left| \frac{y'}{x'} \right| \right)^3 \right] \quad (7)$$

where  $x'$  and  $y'$  are the axis of a coordinate system which is located in the centre of the trajectory. The  $x'$ -axis is in the direction of the initial air flow and the  $y'$ -axis is perpendicular to the  $x'$ -axis. The

proportionality factor  $c_{\text{max}}$  represents the concentration of Helium on the trajectory yielding the following equation:

$$c_{\text{max}} = 100 \cdot (-0.0653 \cdot (\log(4 \cdot \text{Ma}_{\text{air}}^{0.28}))^{-1} \cdot \left[ \frac{x' - x'_p}{d_0} \right]^{0.7}) \quad (8)$$

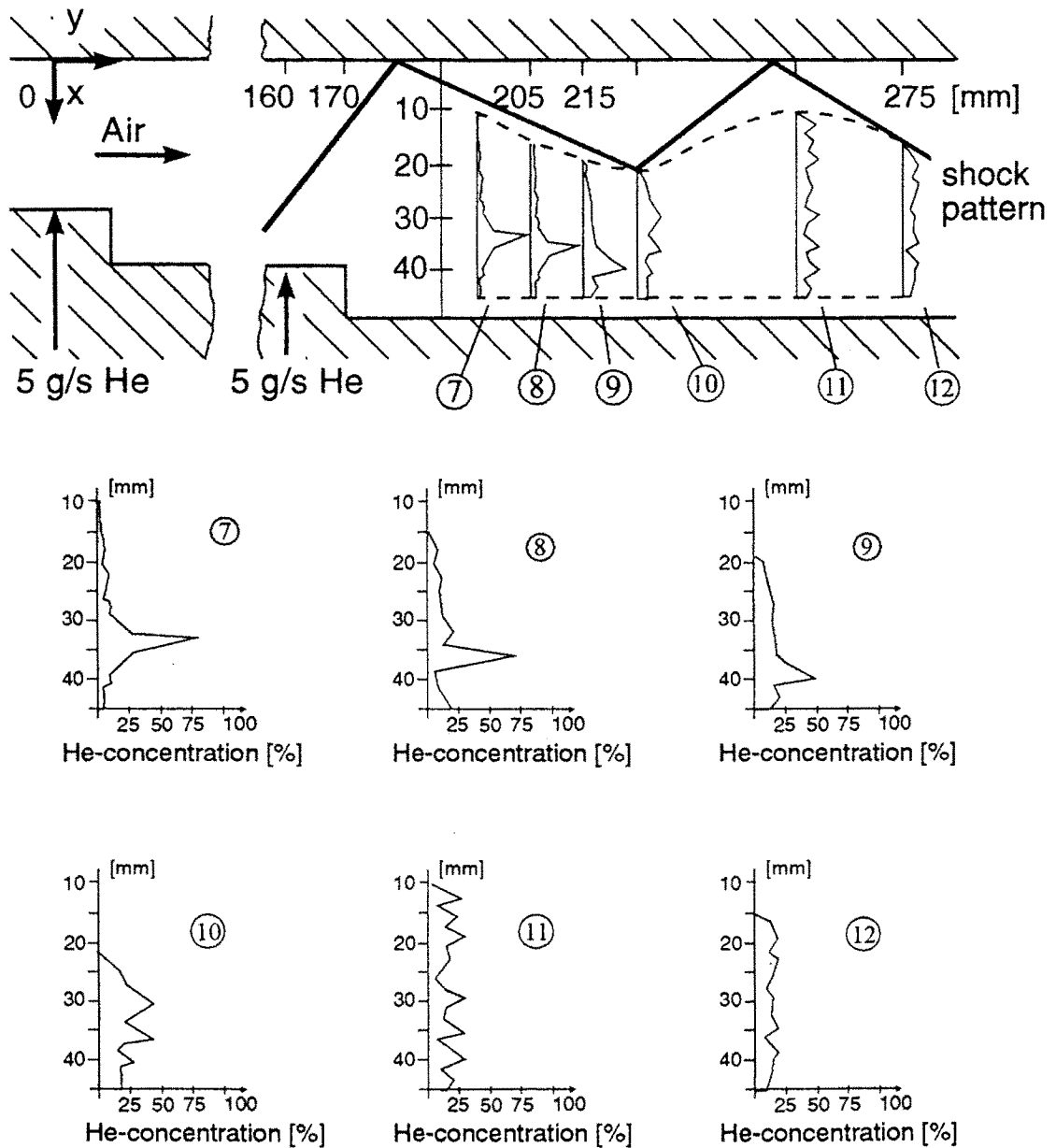


Fig. 8: Influence of multistep injection, shock waves and rearward facing steps on the concentration profile in the mixing jet (four hole injector;  $\text{Ma}_{\text{air}} = 2.1$ ;  $m_{\text{He}} = 10$  g/s)



The coordinate  $x_p'$  indicates the point on the trajectory on which the concentration begins to decrease. This point can be calculated by equation (9).

$$\frac{x_p'}{d_0} = 13.9 \cdot \xi_{\text{He}}^{0.58} \cdot \log \left( 10 \cdot \text{Ma}_{\text{air}}^{0.85} \right) \quad (9)$$

K indicates the gradient of the concentration in the mixing jet perpendicular to the initial air flow. Equation (10) yields the factor for the case of single hole injection.

$$K = 1425 \cdot \xi_{\text{He}}^{0.58} \cdot \log \left[ 10 \cdot \text{Ma}_{\text{air}}^{2.06 \cdot \xi_{\text{He}}^{0.93}} \right] \quad (10)$$

Figure 7 shows the concentration profile of the helium/air mixing jet to demonstrate the influence of shock pattern and cascades of rearward facing steps on the mixing jet. Here the initial air Mach number  $\text{Ma}_{\text{air}}$  was 2.1. The helium was injected perpendicular to the air flow using a four hole injector. The helium mass flow  $m_{\text{He}}$  was 5 g/s. The location of the shocks was taken from shadowgraphs (see Fig. 2). The concentration profile of the mixing jet was measured by means of Raman spectroscopy. It can be seen that the helium/air mixing jet is strongly deformed by the influence of the oblique shock waves. The collision of the reflected shock with the mixing jet leads to a compression of the mixing jet at position 3. After the collision point the helium/air mixing jet expanded extremely due to local gradients in the air flow which are originated by the oblique shock wave. This means that downstream of this point the mixing rate was very high. Large scale vortices in the wake of the second recirculation zone which were induced by the flow around the rearward facing step caused additional turbulent structures in the helium/air mixing jet. This leads again to a strong increase in the mixing rate and to a bigger mixing jet.

For the four hole injector system equation 7 is again used to calculate the concentration distribution in the mixing jet. Nevertheless the evaluations of the experimental data led to different factors. The concentration  $c_{\text{max}}$  on the trajectory is given by equation (11).

$$c_{\text{max}} = 100 \cdot \exp \left( -0.15 \cdot \left[ \log \left( 4 \cdot \text{Ma}_{\text{air}}^{0.71} \right) \right]^{-1} \cdot \left( \frac{x' - x_p'}{d_0} \right)^{0.7} \right) \quad (11)$$

The coordinate  $x_p'$  for the case of four hole injection can be calculated by:

$$\frac{x_p'}{d_0} = 7.6 \cdot \xi_{\text{He}}^{0.58} \cdot \log \left( 10 \cdot \text{Ma}_{\text{air}}^{0.74} \right) \quad (12)$$

Multistep fuel injection. To gain higher mixing rates and a higher penetration of the mixing jet a multistep injection system was used to increase the turbulence-induced convective mass transfer in the mixing jet. Multistep injection means, that fuel is simultaneous injected upstream of the first and of the second rearward facing step. Figure 8 shows the concentration distribution in the mixing jet which was originated using multistep injection. The initial air Mach number  $\text{Ma}_{\text{air}}$  was set to 2.1. The helium was injected perpendicular to the air flow through a four hole injector with a total mass flow rate  $m_{\text{He}}$  of 10 g/s. Similar to the single step injection, the location of the shocks was taken from shadowgraphs and the concentration profile of the mixing jet was measured by means of Raman spectroscopy. Comparing figure 8 with figure 7, it can be seen that the multistep injection causes a higher penetration and a greater thickness of the mixing jet in the wake of the second rearward facing step. This was caused by large scale vortices and an additional impact momentum perpendicular to the air flow due to the second fuel injection. The influence of shock patterns on the development of the mixing jet is approximately the same as for the single step injection. Due to the collision of the reflected shock wave with the fuel jet in the middle of the wake of the rearward facing step the fuel jet became thinner. This indicates that the increase of static pressure caused by the oblique shock wave leads to a suppression of the mixing jet in front and an expansion downstream of the collision point. Due to this there was a increase in the mixing rate down stream of the collision point. Further downstream of this point a homogeneous and large mixing jet with a combustible mixture was measured. This indicates, that the use of rearward facing steps and multistep fuel injection induces turbulent structures and local gradients in the flow field which enhance mixing processes.

### 3.2 Dynamic structure of supersonic hydrogen/air flames

In order to analyse the influence of multistep fuel injection on the structure of supersonic hydrogen/air flames, the experiments concerning the combustion were subdivided into two parts, single and multistep fuel injection. As the concentration of OH-radicals indicate the intensity of chemical reaction in hydrogen/air flames, the structure of the flames and the OH-concentration in the flame front were monitored by means of laser induced fluorescence. Due to the extremely short laser pulse width of 17 ns these flame fronts were chemically and mechanically frozen (see chapter 2.2). This feature and the usage of a thin laser light sheet enabled the two dimensional investigation of turbulent structures in the flame.

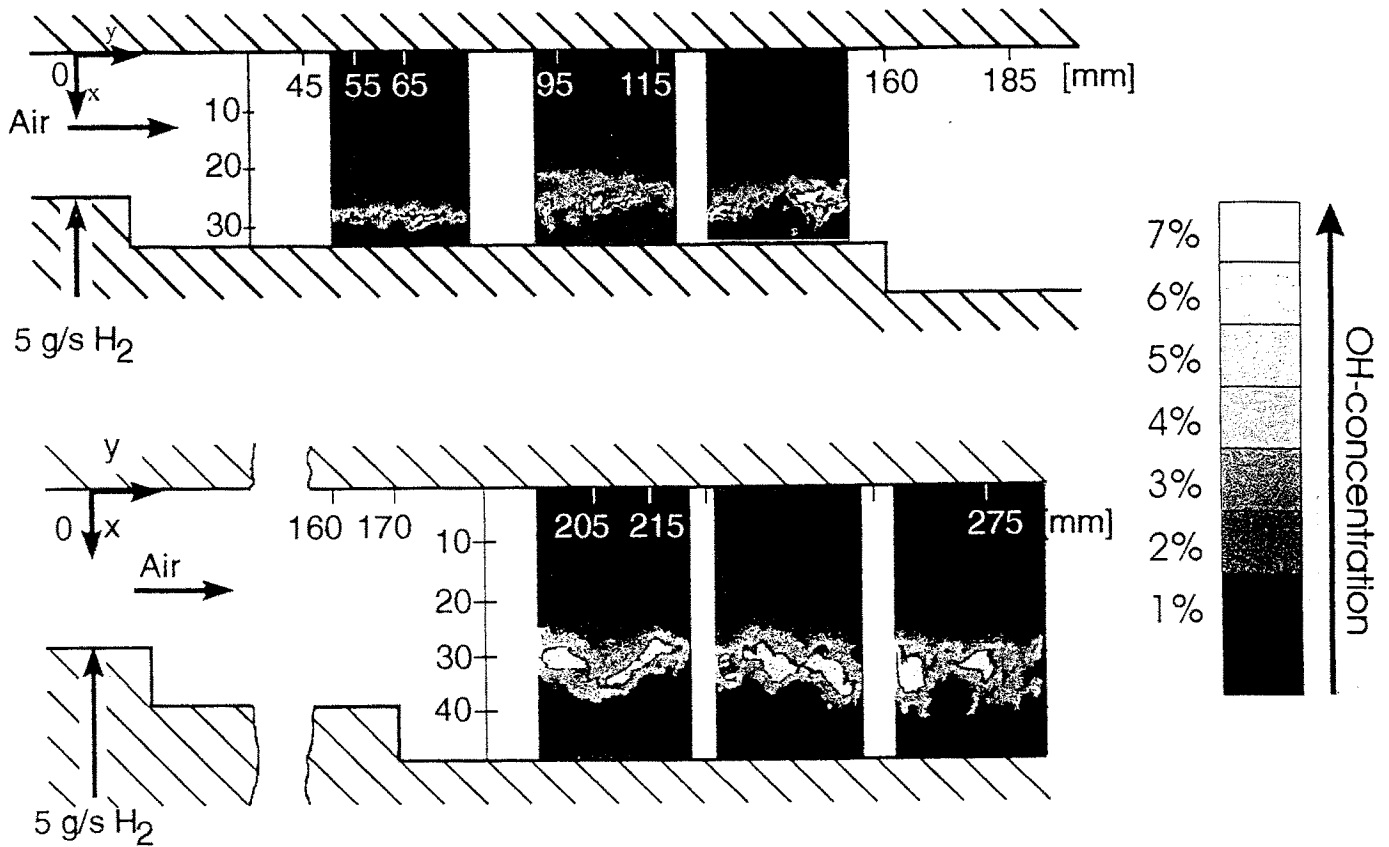


Fig. 9: Turbulent flame structure in the wake of the first and second recirculation zone monitored by means of laser induced fluorescence ( $Ma_{air}=2.1; m_{H_2}=5.0$  g/s; single step injection, four holes)

**Singlestep fuel injection.** Figure 9 shows the turbulent flame structure in the wake of the first and second recirculation zone recorded by means of laser induced fluorescence. Here, the initial air Mach number  $Ma_{air}$  was 2.1. Hydrogen was injected upstream of the first rearward facing step through a row of four injection holes with a mass flow rate  $m_{H_2}$  of 5 g/s. This Figure depicts that the stabilization zone of the flame is located in the free shear layer which separates the mixing jet and the wake of the first rearward facing step. There are the greatest gradients of the velocity and thus there are the highest degrees of turbulence in this shear layer which enhance the mixing process and the flame stabilization. The increasing OH-concentration downstream of the first rearward facing step indicates the increase of the reaction rate in the flame due to turbulence induced mass transfer. Comparing the outer border of the flame with the inner border it can be seen that on the supersonic side the flame was influenced by fine scaled vortices whereas and on the subsonic side in the wake of the recirculation zone the flame was affected by large scale vortices. This means

that due to the higher intensity of turbulence on the supersonic side of the flame these eddies were smaller compared with the eddies on the subsonic side.

The second rearward facing step induced additional turbulent structures in the mixing jet in the wake of the second recirculation zone. This led to an increase in the rate of chemical reaction indicated by the strong increase of OH-concentration in the flame (fig. 9 bottom). Figure 9 also shows that due to the additional turbulence the flame penetrated deeper into the surrounding air flow in the wake of the second rearward facing step. The wavy structure of the flame in the wake of the second rearward facing step is caused by the high intensity of turbulence in the mixing jet which enhanced the combustion process. Here the outer border of the flame was again influenced by fine scaled vortices and the subsonic side is influenced by large scaled eddies.

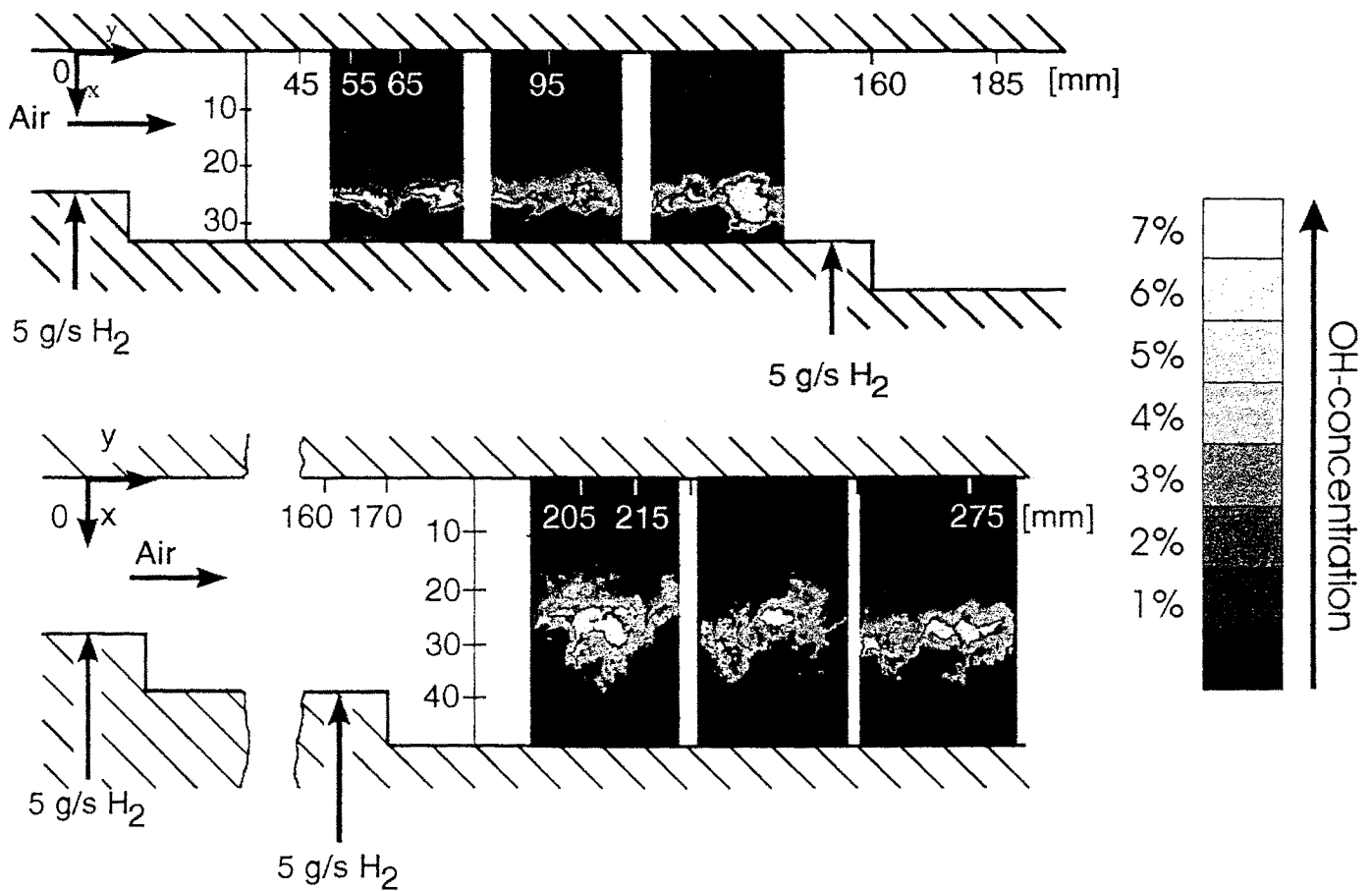


Fig. 10: Turbulent flame structure in the wake of the first and second recirculation zone monitored by means of laser induced fluorescence ( $Ma_{air}=2.1$ ;  $m_{H_2}=10.0$  g/s; multistep injection, four holes)

These results are in very good agreement with the results of the 'cold mixing experiments' shown in the previous chapter.

**Multistep fuel injection.** To gain shorter flame length and higher fuel efficiencies multistep fuel injection was used to generate turbulence in the reaction zone of the flame to increase the reaction rate and to stirring-up the combustion process. Figure 10 shows the structure of the flame and the OH-concentration distribution in the reaction zone in the wake of the first and second rearward facing step. The initial air Mach number  $Ma_{air}$  was set to 2.1. The hydrogen was injected perpendicular to the air flow through a four hole injector upstream of the first and second rearward facing step with a total mass flow rate  $m_{H_2}$  of 10 g/s. It can be seen that in the wake of the first rearward facing step the turbulent structure of the flame is similar to the structure of the flame in the singlestep fuel injection. The influence of the second injection on the flame structure can be seen in the wake of the second rearward facing step. Due to large scaled vortices induced by the second injection the rate of chemical reaction has been increased. This was indicated by the increase in OH-concentration in the reaction zone. Comparing figure 10 with figure 9 it can be seen that

the flame penetrated deeper into the surrounding air flow in the wake of the second rearward facing step. In the mixing jet the reaction zone was more broader than in the singlestep injection experiments caused by the higher intensity of turbulence. All experiments have shown that multistep fuel injection in addition with rearward facing steps provides excellent mixing rate and an increase in the rate of chemical reaction. Thereby it was possible to achieve a short flame length and the conditions of flame stabilization.

#### 4. Summary and Concluding Remarks

A multistep combustor with cascades of rearward facing steps and a multistep injection system was used to investigate the influence of the injector system and the rearward facing steps on the mixing and combustion processes in sub- and supersonic air flames. These experiments were conducted by means of non-intrusive optical measurement techniques. The results showed that oblique shock waves and turbulent structures in the flow field enhance the mixing and combustion processes. The application of multistep injector and rearward facing steps which induces turbulent structures in the reaction zone of the mixing jet led to an increase in the mixing rate and to a stirring-up of

the combustion process. Furthermore by the use of multistep fuel injection it was possible to achieve short flame length.

To describe the growth and the penetration of the mixing jet a power law was developed. Equation (7) in chapter 3.1 provides the capability to calculate the concentration distribution in the mixing jet.

This work will be continued by detailed investigation about the velocity distribution in the flow field and in the wake of the recirculation zones using two beam laser Doppler velocimetry. Furthermore it is planned to measure the major species concentration in the flame and in the exhaust to calculate the combustion efficiency.

### 5. References

1. M. Haibel, F. Mayinger, The effect of turbulent structures on the development of mixing and combustion processes in sub- and supersonic H<sub>2</sub> flames, *Int. J. Heat Mass Transfer*. Vol. 37, Suppl. 1, pp. 241-253
2. M. Oswald, R. Guerra and Waidmann, Investigation of the flow field of a scramjet combustor with parallel hydrogen injection through a strut by particle image displacement velocimetry, *Proceedings of the 3rd International Symposium on special topics in chemical propulsion*, pp. 113-115. The Pennsylvania State University, University Park, PA(1993)
3. R.J. Fuller, R. B. Mays, R. H. Thomas and J. A. Schetz, Mixing studies of helium and air at high supersonic speeds, *AIAA J.* 30,2234-2243 (1992)
4. R. J. Bakos, J. Tamango, O. Rizkalla, M. V. Pulsonetti, W. Chinitz and J. I. Erdos, Hypersonic mixing and combustion studies in the hypulse facility, *J. Propulsion Power* 8, 900-906 (1992)
5. M. P. Lee, B. K. McMillin, J. L. Palmer and R. K. Hanson, Planar fluorescence imaging of transverse jet in supersonic cross flow, *J. Propulsion Power* 8, 729-735 (1992)
6. J. A. Schetz, F. S. Billig and S. Favin, Analysis of slot injection in hypersonic flow, *J. Propulsion Power* 7, 115-122 (1991)
7. J. A. Schetz, R. H. Thomas and P. S. King, Combined tangential-normal injection into supersonic flow, *J. Propulsion Power* 7, 420-430 (1991)
8. E. J. Fuller, R. H. Thomas and J. A. Schetz, Effects of yaw on low angle injection into super-sonic flow, *AIAA paper 91-0014*. American Institute of Aeronautics und Astronautics, Washington, D.C. (1991)
9. M. Takashashi and A. K. Hayashi, Numerical study on the mixing and combustion of injecting hydrogen jets in a supersonic air flow, *AIAA Paper 91-0574*. American Institute of Aeronautics und Astronautics, Washington, D.C. (1991)
10. T. R. A. Bussing and G. L. Lidstone, Transverse fuel injection model for a scramjet propulsion system, *J. Propulsion Power* 6, 355-356 (1990)
11. N. L. Messerschmith, S. G. Goebel, J. P. Remie, J. C. Dutton and H. Krier, Investigation of a supersonic mixing layer, *J. Propulsion Power* 6, 353-254 (1990)
12. J. A. Schetz, R. H. Thomas and f. S. Billig; Gaseous injection in high speed flow, *Proceedings of the Ninth International Symposium on Air Breathing Engines*, Vol. 1, pp. 1-16. American Institute of Aeronautics and Astronautics, Washington, D. C. (1989)
13. J. A. Schetz, S. Favin and F. S. Billig, Simplified analysis of slot injection in hypersonic flow, *AIAA Paper 89-0622*. American Institute of Aeronautics and Astronautics, Washington, D. C. (1988).
14. J. A. Schetz, R. H. Thomas and P. S. King, Combined tangential-normal injection into a supersonic flow, *AIAA Paper 89-0622*. American Institute of Aeronautics and Astronautics, Washington, D. C. (1989)
15. S. C. Lee, Turbulent mixing of coaxial jets between hydrogen and air, *Int. J. Hydrogen Energy* 11, 807-816 (1986)
16. J. A. Schetz, *Injection and Mixing in Turbulent Flow*. American Institute of Aeronautics and Astronautics, New York, (1980)
17. R. C. Rogers, A study of the mixing of hydrogen injected normal to a supersonic airstream, *NASA TN D-6114*, (1971)
18. J. A. Schetz, F. S. Billig, Penetration of Gaseous Jets Injected into a Supersonic Stream, *J. Spacecraft*, Vol 3; No. 11:1658-1555 Nov. 1966

19. W. Hauf and U. Grigull. Optical Methods in Heat Transfer. Academic Press, New York (1970)
20. F. Mayinger and W. Panknin, Holography in heat and mass transfer, International Heat Transfer Conference, Tokyo, Vol. 6, p. 27 (1978)
21. F. Mayinger, Optical Measurement Techniques, Springer, Berlin (1994)
22. M. Haibel, F. Mayinger and G. Strube, Application of non-intrusive diagnostic methods to sub- and supersonic hydrogen/air flames, Proceedings of the 3rd International Symposium on special topics in chemical propulsion, pp. 109-112. The Pennsylvania State University, University Park, PA (1993)
23. F. Mayinger, W. Gabler, Spectroscopic Techniques for Ram-Combustors, Proceedings of the 2nd Space Course on Low Earth Orbit Transportation, Vol. 1 Munich, 1993
24. R. C. Orth and J. A. Funk, An experimental and comparative study of jet penetration in supersonic flow, J. Spacecraft Rockets 4, 1236-1242 (1967)